Radiotherapy and Oncology 183 (2023) 109593

Contents lists available at ScienceDirect

Radiotherapy and Oncology

journal homepage: www.thegreenjournal.com

Original Article

Machine-learning with region-level radiomic and dosimetric features for predicting radiotherapy-induced rectal toxicities in prostate cancer patients

Zhuolin Yang [a,b,*], David J. Noble [c,d], Leila Shelley [a], Thomas Berger [a], Raj Jena [e], Duncan B. McLaren [c,d], Neil G. Burnet [f], William H. Nailon [a,b,g]

[a] Department of Oncology Physics, Edinburgh Cancer Centre, Western General Hospital, Crewe Road South, Edinburgh EH4 2XU; [b] School of Engineering, The University of Edinburgh, The King's Buildings, Mayfield Road, Edinburgh EH9 3JL; [c] Edinburgh Cancer Research Centre, Institute of Genetics and Cancer, The University of Edinburgh, Edinburgh; [d] Department of Clinical Oncology, Edinburgh Cancer Centre, Western General Hospital, Crewe Road South, Edinburgh EH4 2XU; [e] The University of Cambridge, Department of Oncology, Cambridge Biomedical Campus, Hills Road, Cambridge CB2 0QQ; [f] The Christie NHS Foundation Trust, Manchester M20 4BX; and [g] School of Science and Engineering, The University of Dundee, Dundee DD1 4HN, UK

ARTICLE INFO

Article history:
Received 24 March 2022
Received in revised form 27 January 2023
Accepted 24 February 2023
Available online 3 March 2023

Keywords:
Toxicity
Radiotherapy
Prostate cancer
Machine learning
Radiomics

ABSTRACT

Background and purpose: This study aims to build machine learning models to predict radiation-induced rectal toxicities for three clinical endpoints and explore whether the inclusion of radiomic features calculated on radiotherapy planning computerised tomography (CT) scans combined with dosimetric features can enhance the prediction performance.

Materials and methods: 183 patients recruited to the VoxTox study (UK-CRN-ID-13716) were included. Toxicity scores were prospectively collected after 2 years with grade $\geq$ 1 proctitis, haemorrhage (CTCAEv4.03); and gastrointestinal (GI) toxicity (RTOG) recorded as the endpoints of interest. The rectal wall on each slice was divided into 4 regions according to the centroid, and all slices were divided into 4 sections to calculate region-level radiomic and dosimetric features. The patients were split into a training set (75%, N = 137) and a test set (25%, N = 46). Highly correlated features were removed using four feature selection methods. Individual radiomic or dosimetric or combined (radiomic + dosimetric) features were subsequently classified using three machine learning classifiers to explore their association with these radiation-induced rectal toxicities.

Results: The test set area under the curve (AUC) values were 0.549, 0.741 and 0.669 for proctitis, haemorrhage and GI toxicity prediction using radiomic combined with dosimetric features. The AUC value reached 0.747 for the ensembled radiomic-dosimetric model for haemorrhage.

Conclusions: Our preliminary results show that region-level pre-treatment planning CT radiomic features have the potential to predict radiation-induced rectal toxicities for prostate cancer. Moreover, when combined with region-level dosimetric features and using ensemble learning, the model prediction performance slightly improved.

In the UK, prostate cancer (PCa) is the most common cancer in men, resulting in 10,755 deaths in England and Wales in 2017 [1]. Although considered typically a disease of older age, more than a quarter of cases occur before current retirement age. Radiotherapy is used with curative intent in more than half of all PCa patients, and in the last three decades there have been significant technological improvements resulting in new treatment strategies such as image-guided intensity-modulated radiotherapy (IMRT) and stereotactic body radiotherapy (SBRT) [2]. Whilst these approaches can deliver higher radiation doses to tumours, maintain acceptably low doses to surrounding normal tissues, and have been shown in clinical trials to improve treatment outcomes, irradiation to organs at risk (OARs) is still unavoidable, causing complications. Moreover, when planning radiotherapy, coverage of the target areas should not be reduced to avoid irradiation to OARs. Several studies comparing moderate hypofractionation and conventional fractionation for treating PCa patients suggest that long-term side effects are similar, indicating that late toxic effects on the rectum and bladder remain a significant concern [3–5].

There has been research [6–8] that has modelled gastrointestinal (GI) complications using normal tissue complication probability (NTCP) models, which are based on clinical and dosimetric

* Corresponding author at: Department of Oncology Physics, Edinburgh Cancer Centre, Western General Hospital, Crewe Road South, Edinburgh EH4 2XU, UK.

E-mail address: Zhuolin.Yang@ed.ac.uk (Z. Yang).

https://doi.org/10.1016/j.radonc.2023.109593
0167-8140/

data. However, there are large uncertainties when using these radiobiological-based models and their associated parameters on different patient cohorts with unique characteristics, which makes generalisability and reproducibility difficult. Moreover, dose-volume histogram (DVH)-based models discard spatial dose information, which may be vital for identifying significant toxicity in patients [9,10]. In addition to NTCP modelling, many studies [11–13] have correlated radiotoxicity with clinical and dosimetric parameters using statistical analysis and machine learning. Nevertheless, the limitation of these models is that they do not consider the individual patient response to radiotherapy. Since a patient's radiosensitivity is dependent on a complex blend of genotype and phenotype parameters, there is growing interest in developing predictive biomarkers for treatment personalisation. One very promising area is radiomics, interest in which has grown steadily over the past few years [14–16]. The concept of predicting radiotoxicity using radiomics is based on the hypothesis that image features can reflect underlying physio-pathological information. Additionally, radiomics can capture tumour and organ-specific intrinsic heterogeneity, which can be used to assess individual susceptibility to radiotoxicity, enabling further progress in personalised medicine [17,18].

However, while there have been several studies applying radiomics analysis of different medical images and correlating radiomic features with dose factors to facilitate the development of personalised therapy, there has been limited research investigating the relationship between pre-treatment planning computerised tomography (CT) radiomic features and late rectal toxicity induced by PCa radiotherapy. In this study, we aim to explore whether region-level pre-treatment planning CT radiomic features of the rectal wall correlate with three of the most common late toxicity endpoints, namely haemorrhage, proctitis and GI toxicity.

Materials and methods

Patients

The patient data (N = 187) used for this analysis was prospectively and rigorously collected as part of the UK Clinical Research Network Study Portfolio (UK-CRN-ID-13716) VoxTox study, details of which have previously been published [10,19–21]. VoxTox received approval from the National Research Ethics Service (NRES) Committee East of England (13/EE/0008) in February 2013. Appropriate consent was obtained from all participants. The goal of the programme was to link the accumulated dose at voxel level with toxicity outcomes [22]. Of the 187 patients, 4 were excluded during data processing to avoid generating null feature sets from some regions of rectal wall leaving a total of 183 patients. All patients were treated with helical TomoTherapy (Accuray Inc., Sunnyvale, CA, USA), including daily image guidance megavoltage (MV) CT with positional correction before treatment [19]. The acquisition parameters of the kilovoltage (kV) CT planning scans are listed in Supplementary Material A. To investigate the potential predictive power of pre-treatment planning CT radiomic features, three commonly observed late toxicities were recorded two years after the treatment completion using a toxicity questionnaire specifically designed for the VoxTox study, where proctitis and haemorrhage were assessed based on the Common Terminology Criteria for Adverse Events version 4.03 (CTCAEv4.03) [23], and GI toxicity was evaluated according to the Radiation Therapy Oncology Group (RTOG) scoring system [24]. The incidence rates at 2 years for all clinical endpoints are shown in Table 1. All calculations were performed using Python 3.7.13 (Python Software Foundation, OR, USA).

Fractionation schedules

Patients included in the analysis were assigned to two fractionation schedules, N = 107 with 74 Gy in 37 fractions and N = 76 with 60 Gy in 20 fractions. The doses for the patients prescribed 60 Gy in 20 fractions were converted to equivalent dose in 37 fractions using the tissue-specific biological response α/β = 2.1 Gy based on CHHiP (Conventional versus hypofractionated high-dose intensity-modulated radiotherapy for prostate cancer: 5-year outcomes of the randomised, non-inferiority, phase 3 CHHiP trial) constraints and used previously in other VoxTox studies with equivalent levels of cumulative toxicity incidence assumed between the two schedules [25,5].

Region-of-interest delineation

All the pre-treatment planning CT scans were manually contoured by an experienced site-expert clinical oncologist following the VoxTox protocols [25]. Since the rectum is a hollow organ where the lumen contains meaningless dosimetric and radiomic information, the rectal wall was selected as the volume of interest and was extracted on each slice by expanding the rectum contour inwards by 2 pixels. Additionally, to incorporate spatial information with radiomic and dosimetric features, a new method was defined to extract regions of interest from the rectal wall. As shown in Fig. 1, in the axial direction, slices for each patient were divided into 4 sections and on each slice the rectal wall was equally divided into 4 regions according to the centroid.

Feature extraction

For each region, subimages of size 8x8 pixels^2 were extracted at 1-pixel intervals after expanding the 2-pixel-wide rectal wall both anteriorly and posteriorly by 3 pixels, and 7 radiomics/texture analysis methods were used to extract a total of 118 features from each region. Details of the radiomic features used are shown in Supplementary Material B. All feature extraction algorithms were implemented adhering to the protocols set out by Image Biomarker Standardization Initiative (IBSI) [26]. To reduce computation time without loss of accuracy, grey-level information from the subimages was quantised to 16 levels before calculating image features [27,28]. After extraction in each region, features were averaged to obtain the region-level radiomic features. The maximum and the mean dose from each region were calculated based on the original dose plan and thereafter referred to as region-level dosimetric features. All the averaged radiomic features, maximum dose and mean dose from 4 regions were combined together as the input of machine learning models. Features with zero variance were removed. All the features were standardised (mean = 0, SD = 1) before further processing.

Feature selection

To avoid overfitting, feature selection algorithms including principal component analysis (PCA), variance threshold, correlation threshold and random forest (RF) importance were applied to the training set to select the most important features and remove highly-correlated and/or redundant features. For PCA, 95%, 90%, 85%, 80% explained variances were used, and for variance threshold, features with variance less than 5, 10, 20, 30 and 40 were removed. For correlation threshold, the correlation coefficient > 0.8 was used to ensure that all selected features do not have a strong linear relationship with one another. For RF importance, 30, 40, 50 and 60 features were selected respectively after feature ranking for the radiomic/radiomic-dosimetric model and 5, 10, 15, 20 features were selected for the dosimetric model.

Table 1
Incidence rates at 2 years for the full VoxTox Prostate dataset, training set and test set, stratified by prescribed dose.

Toxicity Endpoint	Total patients, N(%)	74 Gy, N (%)	60 Gy, N (%)	Training set, N (%)	74 Gy, N (%)	60 Gy, N (%)	Test set, N (%)	74 Gy, N (%)	60 Gy, N (%)
	183 (100)	107 (58)	76 (42)	137 (75)			46 (25)		
Proctitis					82 (60)	55 (40)		25 (54)	21 (46)
= G0	148 (81)	89 (49)	59 (32)	111 (81)	68 (50)	43 (31)	37 (80)	21 (46)	16 (35)
≥ G1	35 (19)	18 (10)	17 (9)	26 (19)	14 (10)	12 (9)	9 (20)	4 (9)	5 (11)
Haemorrhage					78 (57)	59 (43)		29 (63)	17 (37)
= G0	122 (67)	76 (42)	46 (25)	91 (66)	56 (41)	35 (26)	31 (67)	20 (43)	11 (24)
≥ G1	61 (33)	31 (17)	30 (16)	46 (34)	22 (16)	24 (18)	15 (33)	9 (20)	6 (13)
GI Toxicity					78 (57)	59 (43)		29 (63)	17 (37)
= G0	86 (47)	51 (28)	35 (19)	64 (47)	36 (26)	28 (20)	22 (48)	15 (33)	7 (15)
≥ G1	97 (53)	56 (31)	41 (22)	73 (53)	42 (31)	31 (23)	24 (52)	14 (30)	10 (22)

GI: gastrointestinal.

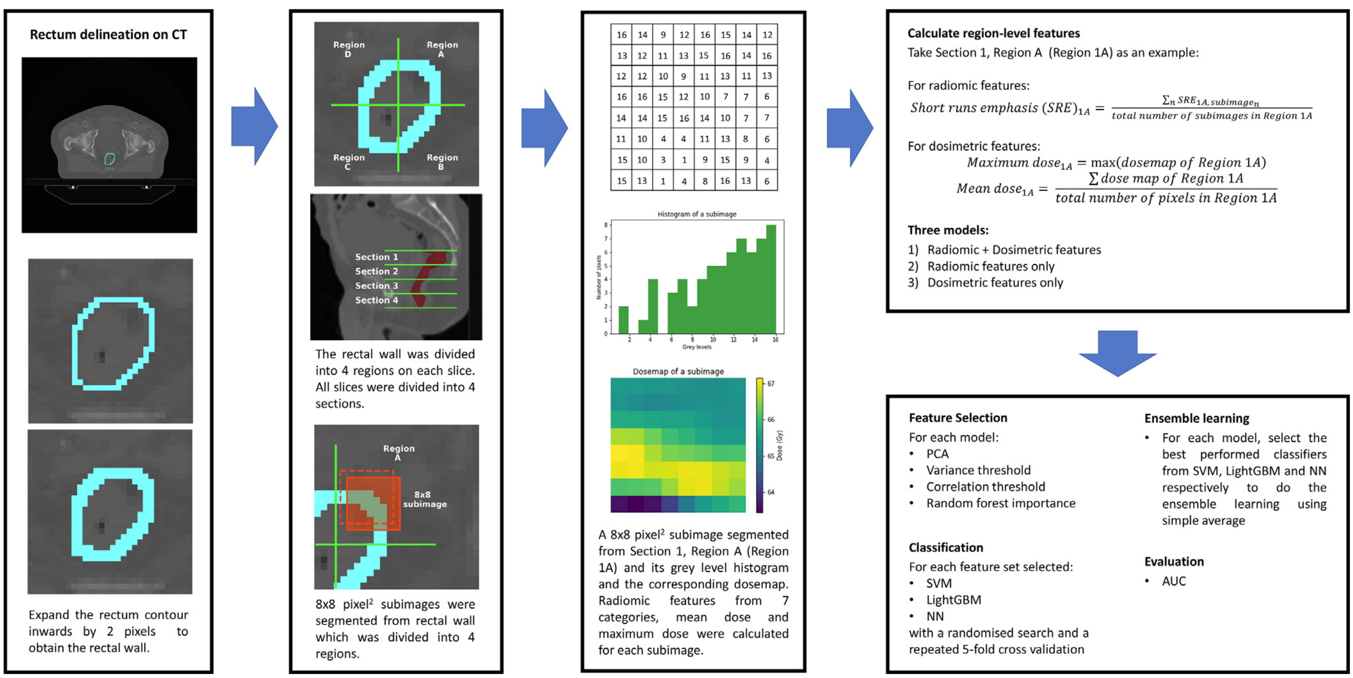

Fig. 1. A diagram illustrating the main steps in building the predictive models using radiomic and dosimetric features extracted from pre-treatment planning CT scans.

Classification

183 patients were split into a training set (75%, N = 137) and a test set (25%, N = 46) with a balanced toxicity incidence rate (Table 1). Radiomic features and dosimetric features were used alone or in combination as the input to a support vector machine (SVM), a light gradient boosting machine (LightGBM) and a neural network (NN). Hyperparameters of the classifiers were fitted using a randomised search with 200 iterations. For each iteration, a 5-fold cross-validation with 20 repetitions was performed. The mean validation area under the curve (AUC) value was calculated by averaging over all folds for each hyperparameter combination and the combination with the highest AUC value was selected as the optimised hyperparameters. The core codes of the classifiers with the optimised hyperparameters are provided in Supplementary Material C. Ensemble learning was applied to improve the performance by averaging the predicted probabilities obtained from different classifiers. AUC of the receiver operator characteristic (ROC) curve and 95% confidence intervals (CIs) were calculated with bootstrap resampling 1000 times. One-sided Mann-Whitney U rank tests were used to compare the predictive performance of different models.

Results

The results of the best models for grade ≥ 1 proctitis, haemorrhage and GI toxicity, selected by mean AUC values of the validation set, are shown in Table 2. The test AUC scores of the selected radiomic, dosimetric and radiomic-dosimetric models for proctitis were 0.431 (95% CI 0.393–0.469), 0.538 (95% CI 0.507–0.568) and 0.549 (95% CI 0.515–0.583), respectively. For haemorrhage, the radiomic-dosimetric model was found to be a highly predictive model with 0.741 (95% CI 0.719–0.762) test AUC, followed by the radiomic model with 0.676 (95% CI 0.653–0.699) AUC and dosimetric model least good with 0.650 (95% CI 0.622–0.678) AUC. For GI toxicity, the test AUC values for radiomic, dosimetric and radiomic-dosimetric models were 0.634 (95% CI 0.610–0.658), 0.573 (95% CI 0.547–0.598) and 0.669 (95% CI 0.645–0.694). For each endpoint, the predictive performance of the radiomic-dosimetric model was compared with that of the radiomic model and the dosimetric model, respectively, using a Mann-Whitney U rank test, with the alternative hypothesis that the distribution underlying the AUC values of the radiomic-dosimetric model is stochastically greater than that of the radiomic model and the dosimetric model ($p < 0.05$). For all endpoints, the

Table 2
Models' performance for the grade ≥ 1 proctitis, haemorrhage and GI toxicity prediction.

Endpoint	Model	Classifier	Feature Selection	Validation AUC (95% CI)	Test AUC (95% CI)	p-value (vs RD)
Proctitis	RD	NN	RF40	0.693 (0.650–0.736)	0.549 (0.515–0.583)	
	R	LGBM	RF50	0.700 (0.654–0.746)	0.431 (0.393–0.469)	<0.001
	D	SVM	Corr0.8	0.609 (0.567–0.651)	0.538 (0.507–0.568)	<0.001
Haemorrhage	RD	LGBM	RF40	0.755 (0.722–0.788)	0.741 (0.719–0.762)	
	R	LGBM	RF30	0.690 (0.653–0.727)	0.676 (0.653–0.699)	<0.001
	D	NN	RF20	0.715 (0.677–0.753)	0.650 (0.622–0.678)	<0.001
GI Toxicity	RD	SVM	RF50	0.744 (0.713–0.755)	0.669 (0.645–0.694)	
	R	LGBM	RF40	0.703 (0.671–0.735)	0.634 (0.610–0.658)	<0.001
	D	SVM	RF10	0.691 (0.657–0.725)	0.573 (0.547–0.598)	<0.001

AUC: area under the curve; CI: confidence interval; GI: gastrointestinal; RD: radiomic-dosimetric model; R: radiomic model; D: dosimetric model; NN: neural network; LGBM: light gradient boosting machine; SVM: support vector machine; RF40: top 40 features from random forest importance; RF50: top 50 features from random forest importance; Corr0.8: correlation threshold = 0.8; RF30: top 30 features from random forest importance; RF20: top 20 features from random forest importance; RF10: top 10 features from random forest importance.

Table 3
AUC values of the ensembled radiomic-dosimetric models for grade ≥ 1 proctitis, haemorrhage and GI toxicity prediction.

Endpoint	Classifier	Validation AUC (95% CI)	Test AUC (95% CI)	Ensembled AUC (95% CI)	p-value
Proctitis	SVM	0.668 (0.618–0.718)	0.548 (0.511–0.585)	0.596	
ensembled RD	LGBM	0.666 (0.622–0.710)	0.541 (0.516–0.567)	(0.561–0.631)	<0.001
	NN	0.693 (0.650–0.736)	0.549 (0.515–0.583)		
Haemorrhage	SVM	0.712 (0.678–0.746)	0.667 (0.641–0.693)	0.747	
ensembled RD	LGBM	0.755 (0.722–0.788)	0.741 (0.719–0.762)	(0.723–0.772)	<0.001
	NN	0.700 (0.665–0.735)	0.695 (0.672–0.718)		
GI Toxicity	SVM	0.744 (0.713–0.755)	0.669 (0.645–0.694)	0.671	
ensembled RD	LGBM	0.689 (0.660–0.718)	0.667 (0.643–0.690)	(0.647–0.694)	0.243
	NN	0.719 (0.689–0.749)	0.656 (0.632–0.681)		

AUC: area under the curve; CI: confidence interval; RD: radiomic-dosimetric model; GI: gastrointestinal; SVM: support vector machine; LGBM: light gradient boosting machine; NN: neural network.

predictive performance of the radiomic-dosimetric models was proven to be statistically superior to that of models using only radiomic or dosimetric features ($p < 0.001$). To establish the relative importance of the radiomic-dosimetric models presented in Table 2, correlated or redundant features were identified and removed prior to prediction using feature selection algorithms. The results of this are shown in Supplementary Material D. Following prediction, the final feature rankings were calculated using the Shapely Additive Explanation (SHAP) approach (Supplementary Material E).

For ensemble learning which averages the prediction probabilities obtained from different classifiers with the highest validation

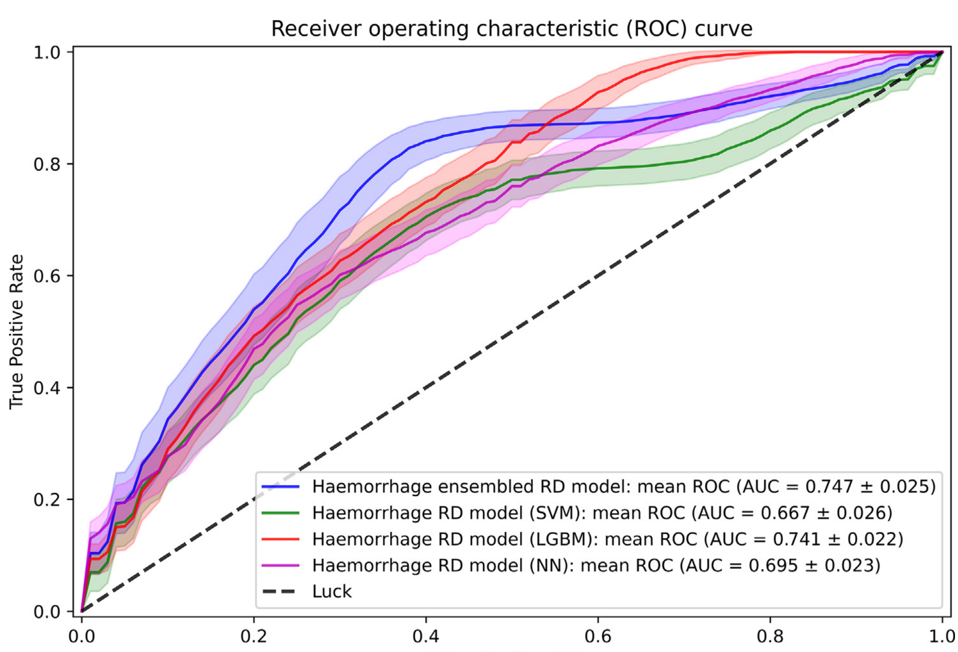

Fig. 2. ROC curves with 95% confidence intervals of the radiomic-dosimetric models and the ensembled radiomic-dosimetric model for grade ≥ 1 haemorrhage prediction.

AUC values, the ensembled radiomic-dosimetric models for proctitis (AUC = 0.596, 95% CI 0.561–0.631) and haemorrhage (AUC = 0.747, 95% CI 0.723–0.772) were found to perform statistically better than using only individual classifiers ($p < 0.001$) (Table 3). For GI toxicity, although the mean AUC value of ensemble learning (AUC = 0.671, 95% CI 0.647–0.694) was greater than the test AUC values obtained from individual classifiers, this improvement was not statistically significant. The ROC curves of the radiomic-dosimetric models for haemorrhage and the ensembled radiomic-dosimetric model with 95% CIs are shown in Fig. 2.

Discussion

Building accurate predictive models for identifying potential patients who may have side effects after radiotherapy may help clinicians decide the best treatment plan for patients. The main goal of the study was to correlate region-level CT radiomic features with late rectal toxicities for PCa radiotherapy and to investigate whether the inclusion of region-level radiomic features together with dosimetric features can enhance prediction performance. In the study, we developed predictive models for mild proctitis, haemorrhage and GI toxicity based on radiomic features, dosimetric features and the combination of radiomic with dosimetric features. The overall trend of these results is that this approach could be helpful to learn more about the predictive power of radiotherapy planning CT radiomic features which can be extracted before the start of the course of treatment. Therefore, at least in theory, they could be used to modify and further individualise the radiotherapy treatment plan.

For haemorrhage and GI toxicity, the radiomic models had test AUCs > 0.63, which showed the feasibility of using planning CT radiomic features for radiotoxicity prediction. After adding radiomic features, compared to using only dosimetric features, the mean AUC values of the test set increased from 0.538 (for proctitis), 0.650 (for haemorrhage) and 0.573 (for GI toxicity) to 0.549, 0.741 and 0.669, representing a marked increase. Besides, the statistical analysis revealed that using the combined feature set significantly improved outcomes for all endpoints. Although the prediction results for proctitis obtained by individual classifiers were not satisfactory, the AUC value of the ensembled radiomic-dosimetric model for proctitis almost reached 0.6. Additionally, the AUC values significantly improved for proctitis and haemorrhage by utilising ensemble learning which aggregates the predictions from multiple different classifiers, and thus reduces overfitting and improves the generalisability [29]. Of the three endpoints, haemorrhage had the best results, with a much smaller difference between the validation AUC and the test AUC compared to proctitis and GI toxicity because haemorrhage is a more objective and reproducible endpoint. Although there are well-established toxicity scoring systems, predicting adverse events is challenging as perceptions and situations may vary for different patients, and thus the patient-reported toxicity data remains subjective.

Several investigators have demonstrated the good performance of machine learning models in predicting rectal toxicities [14,30,31]. Gulliford et al. [30] used artificial neural networks (ANNs) with clinical and dosimetric data to predict RTOG G2/G3 rectal bleeding in 119 PCa patients after radiotherapy. The results were encouraging with sensitivity and specificity of above 55%. Tomatis et al. [31] correlated dosimetric and clinical features with SOMA/LENT (subjective, objective, management and analytic/late effects of normal tissue) G2 rectal bleeding in 718 PCa patients using ANNs and had AUC = 0.714. In line with our study, some researchers have also aimed to correlate radiomics with toxicity outcomes [14–16]. Abdollahi et al. [16] analysed 33 patients and correlated the change of rectal wall magnetic resonance imaging (MRI) radiomic features with early rectal toxicity. An AUC of 0.81 was reached when all significant features were combined, suggesting that pre-treatment MRI features could predict early rectal toxicity for PCa radiotherapy. Later, Abdollahi et al. [15] associated image texture changes on pre- and post-treatment T2-weighted MRI of the rectal wall with radiation dose and urinary toxicity in 33 patients. The results showed a good correlation between feature changes and urinary toxicity. Mostafaei et al. [14] analysed the CT image features from 64 PCa patients using a stacking regression algorithm to predict acute cystitis and proctitis. No external validations were applied in these studies. The findings of the research are encouraging. However, their results are limited by the relatively small numbers of patients and by the fact that the IBSI processes, which promote reproducibility and standardisation across the field [32], were not followed [26].

One key implication of the results, that radiomic features derived from the planning CT can improve the prediction of toxicity, is that toxicity could be further mitigated by acting on the predictions. For example, men with predicted high risks of toxicity could be re-planned with more strict planning dosimetry objectives, and they could be selected for adaptive treatment based on accumulated rectal dose [21] or offered insertion of a rectal gel spacer. In addition, radiomic features may be detecting indicators of underlying biological mechanisms of toxicity and could direct further research into the fundamental biology of toxicity [33].

Although the results of this study are encouraging, there are limitations. Firstly, this study was conducted in a single institution. Although the data was collected prospectively following a carefully designed protocol, and the diversity of the dataset have been reflected by repeated cross-validation with different splits of the data, further studies with larger datasets obtained from multiple institutions would be required to demonstrate the generalisability of the results. Second, it is necessary to perform multiple experiments to investigate robust and reproducible radiomic features and to combine these with other informative variables such as patient characteristics and biological factors including genotype [33] to realise personalised treatment. The last limitation is that this study is conducted to predict only G1 late rectal toxicities because of the low incidence of G2-3 toxicities and more work must be done to build models for moderate/severe late rectal toxicities such as in the previous VoxTox study by Shelley et al. [21]. That said, G1 toxicity is an important consideration for patients receiving radiotherapy and all efforts to reduce even G1 toxicities will be welcomed by patients.

There are several studies investigating the power of radiomics on toxicity prediction based on statistical analysis. Radiomic features extracted from grey level co-occurrence matrix (GLCM) and grey level run length matrix (GLRLM) on MRI were found to have a strong correlation with structural changes in the rectal wall during PCa radiotherapy [16]. Similar findings were reported in another study where GLCM features calculated on MRI were observed to be correlated with bladder wall changes during PCa radiotherapy[15]. In studies of radiation therapy for other cancers, short run emphasis from GLRLM and maximum CT intensity extracted on planning CT scans were found to significantly improve the prediction of xerostomia and sticky saliva in head and neck cancer patients [34,32]. Changes in first-order statistics (FOS) and GLCM features during oesophageal cancer radiotherapy were also reported to be correlated with G3 radiation pneumonitis (CTCAEv4). Although the goal of this study was to build predictive models based on machine learning algorithms rather than carrying out a feature-level analysis, further studies will be conducted to identify robust imaging biomarkers for the prediction of radiation-induced late rectal toxicity. Moreover, radiomic-level analysis incorporating daily imaging information from image guidance scans will be conducted to investigate possible differences between conventional fractionation and hypofractionation in future work.

Region-level radiomic pre-treatment planning CT texture analysis is a promising approach for rectal toxicity modelling in PCa radiotherapy. In addition, these models may help in the development of individualised treatment planning for PCa radiotherapy and offer clinicians new insight into treatment risks.

Conflicts of Interest

None.

Acknowledgment

The authors are grateful for the support of 1) the VoxTox and computational Oncology group at the University of Cambridge, 2) the PROSECCA team at the Edinburgh Cancer Centre and 3) the staff in the Department of Oncology Physics at the Edinburgh Cancer Centre and the Institute for Digital Communications, College of Science and Engineering at the University of Edinburgh. VoxTox was supported by a CRUK grant (ref C8857\A13405) with ethics approval: 13/EE/0008. The work was generously supported by the Chief Scientist Office (CSO) Scotland grant (TCS/17/26 - CSO Award), IMAGE-INE: Analysing IMAGE guIdance scaNs to prEdict late toxicity after radiotherapy in head and neck cancer patietns. This study was also kindly supported by the prostate cancer UK (PCUK) grant (MA-CT20-010), PROSECCA: Improving radiotherapy in PROState cancer using EleCtronic population-based healthCAre data: The PROSECCA study, answering new questions in prostate cancer.

Appendix A. Supplementary material

Supplementary data to this article can be found online at https://doi.org/10.1016/j.radonc.2023.109593.

References

[1] Deaths from prostate cancer, England and Wales, 2001 to 2017; 2019. https://www.ons.gov.uk/peoplepopulationandcommunity/birthsdeathsandmarriages/deaths/adhocs/009669deathsfromprostatecancerenglandandwales2001to2017. Accessed 16 May 2022.
[2] Berger T, Noble DJ, Shelley LEA, et al. 50 years of radiotherapy research: Evolution, trends and lessons for the future. Radiot Oncol 2021;165:75–86. https://doi.org/10.1016/j.radonc.2021.09.026.
[3] Yang F, Ghosh S, Yee D, et al. Patient-Reported Outcomes in a Prostate Cancer Hypofractionation Trial. Int J Radiat Oncol 2022. https://doi.org/10.1016/j.ijrobp.2022.04.045.
[4] Arcangeli G, Saracino B, Arcangeli S, et al. Moderate hypofractionation in high-risk, organ-confined prostate cancer: Final results of a phase III randomized trial. J Clin Oncol 2017;35:1891–7. https://doi.org/10.1200/JCO.2016.70.4189.
[5] Dearnaley D, Syndikus I, Mossop H, et al. Conventional versus hypofractionated high-dose intensity-modulated radiotherapy for prostate cancer: 5-year outcomes of the randomised, non-inferiority, phase 3 CHHiP trial. Lancet Oncol 2016;17:1047–60. https://doi.org/10.1016/S1470-2045(16)30102-4.
[6] Pedersen J, Liang X, Casares-Magaz O, et al. Multivariate normal tissue complication probability models for rectal and bladder morbidity in prostate cancer patients treated with proton therapy. Radiother Oncol 2020;153:279–88. https://doi.org/10.1016/j.radonc.2020.10.025.
[7] Schaake W, van der Schaaf A, van Dijk LV, et al. Normal tissue complication probability (NTCP) models for late rectal bleeding, stool frequency and fecal incontinence after radiotherapy in prostate cancer NTCP models for anorectal side effects patients. Radiother Oncol 2016;119:381–7. https://doi.org/10.1016/j.radonc.2016.04.005.
[8] Gulliford SL, Partridge M, Sydes MR, et al. Parameters for the Lyman Kutcher Burman (LKB) model of Normal Tissue Complication Probability (NTCP) for specific rectal complications observed in clinical practise. Radiother Oncol 2012;102:347–51. https://doi.org/10.1016/j.radonc.2011.10.022.
[9] Marks LB, Yorke ED, Jackson A, et al. Use of normal tissue complication probability models in the clinic. Int J Radiat Oncol 2010;76:S10–9. https://doi.org/10.1016/j.ijrobp.2009.07.1754.
[10] Shelley LEA, Sutcliffe MPF, Thomas SJ, et al. Associations between voxel-level accumulated dose and rectal toxicity in prostate radiotherapy. Phys Imaging Radiat Oncol 2020;14:87–94. https://doi.org/10.1016/j.phro.2020.05.006.
[11] Pan X, Levin-Epstein R, Huang J, et al. Dosimetric predictors of patient-reported toxicity after prostate stereotactic body radiotherapy: Analysis of full range of the dose-volume histogram using ensemble machine learning. Radiother Oncol 2020;148:181–8. https://doi.org/10.1016/j.radonc.2020.04.013.
[12] Carrara M, Massari E, Cicchetti A, et al. Development of a ready-to-use graphical tool based on artificial neural network classification: application for the prediction of late Fecal incontinence after prostate cancer radiation therapy. Int J Radiat Oncol 2018;102:1533–42. https://doi.org/10.1016/j.ijrobp.2018.07.2014.
[13] Fargeas A, Acosta O, Ospina Arrango JD, et al. Independent component analysis for rectal bleeding prediction following prostate cancer radiotherapy. Radiother Oncol 2018;126:263–9. https://doi.org/10.1016/j.radonc.2017.11.011.
[14] Mostafaei S, Abdollahi H, Kazempour Dehkordi S, et al. CT imaging markers to improve radiation toxicity prediction in prostate cancer radiotherapy by stacking regression algorithm. Radiol Medica 2020;125:87–97. https://doi.org/10.1007/s11547-019-01082-0.
[15] Abdollahi H, Tanha K, Mofid B, et al. MRI radiomic analysis of IMRT-induced bladder wall changes in prostate cancer patients: A relationship with radiation dose and toxicity. J Med Imaging Radiat Sci 2019;50:252–60. https://doi.org/10.1016/j.jmir.2018.12.002.
[16] Abdollahi H, Mahdavi SR, Mofid B, et al. Rectal wall MRI radiomics in prostate cancer patients: prediction of and correlation with early rectal toxicity. Int J Radiat Biol 2018;94:829–37. https://doi.org/10.1080/09553002.2018.1492756.
[17] Gillies RJ, Kinahan PE, Hricak H. Radiomics: Images are more than pictures, they are data. Radiology 2016;278:563–77. https://doi.org/10.1148/radiol.2015151169.
[18] Gardin I, Grégoire V, Gibon D, et al. Radiomics: Principles and radiotherapy applications. Crit Rev Oncol Hematol 2019;138:44–50. https://doi.org/10.1016/j.critrevonc.2019.03.015.
[19] Burnet NG, Adams EJ, Fairfoul J, et al. Practical aspects of implementation of helical tomotherapy for intensity-modulated and image-guided radiotherapy. Clin Oncol 2010;22:294–312. https://doi.org/10.1016/j.clon.2010.02.003.
[20] Burnet NG, Scaife JE, Romanchikova M, et al. Applying physical science techniques and CERN technology to an unsolved problem in radiation treatment for cancer: The multidisciplinary 'VoxTox' research programme. Cern IdeaSquare J Exp Innov 2017;1:3–12. https://doi.org/10.23726/cij.2017.457.
[21] Shelley LEA, Scaife JE, Romanchikova M, et al. Delivered dose can be a better predictor of rectal toxicity than planned dose in prostate radiotherapy. Radiother Oncol 2017;123:466–71. https://doi.org/10.1016/j.radonc.2017.04.008.
[22] Scaife JE, Thomas SJ, Harrison K, et al. Accumulated dose to the rectum, measured using dose-volume histograms and dose-surface maps, is different from planned dose in all patients treated with radiotherapy for prostate cancer. Br J Radiol 2015;88. https://doi.org/10.1259/bjr.20150243.
[23] Cancer Institute N. Common Terminology Criteria for Adverse Events; 2020.
[24] Pilepich MV, Asbell SO, Krall JMD, et al. Correlation of radiotherapeutic parameters and treatment related morbidity-analysis of RTOG study. 1987:77–06.
[25] Shelley LEA. Accumulating delivered dose to the rectum to improve toxicity prediction in prostate radiotherapy PhD. University of Cambridge; 2019. p. 2019.
[26] Zwanenburg A, Vallières M, Abdalah MA, et al. The image biomarker standardization initiative: Standardized quantitative radiomics for high-throughput image-based phenotyping. Radiology 2020;295:328–38. https://doi.org/10.1148/radiol.2020191145.
[27] Montgomery D. Improving radiotherapy using image analysis and machine learning. 2015.
[28] Hernández M del CV, González-Castro V, Chappell FM, et al. Application of texture analysis to study small vessel disease and blood-brain barrier integrity. Front Neurol 2017;8. https://doi.org/10.3389/fneur.2017.00327.
[29] Ganaie MA, Hu M, Tanveer* M, Suganthan* PN, Ensemble deep learning: A review. 2021.
[30] Gulliford SL, Webb S, Rowbottom CG, et al. Use of artificial neural networks to predict biological outcomes for patients receiving radical radiotherapy of the prostate. Radiother Oncol 2004;71:3–12. https://doi.org/10.1016/j.radonc.2003.03.001.
[31] Tomatis S, Rancati T, Fiorino C, et al. Late rectal bleeding after 3D-CRT for prostate cancer: Development of a neural-network-based predictive model. Phys Med Biol 2012;57:1399–412. https://doi.org/10.1088/0031-9155/57/5/1399.
[32] Berger T, Noble DJ, Yang Z, et al. Assessing the generalisability of radiomics features previously identified as predictive of radiation-induced sticky saliva and xerostomia. Phys Imaging Radiat Oncol 2023;25:100404. https://doi.org/10.1016/j.phro.2022.12.001.
[33] Kerns SL, Fachal L, Dorling L, et al. Radiogenomics consortium genome-wide association study meta-analysis of late toxicity after prostate cancer radiotherapy. J Natl Cancer Inst 2020;112:179–90. https://doi.org/10.1093/JNCI/DJZ075.
[34] van Dijk LV, Brouwer CL, van der Schaaf A, et al. CT image biomarkers to improve patient-specific prediction of radiation-induced xerostomia and sticky saliva. Radiother Oncol 2017;122:185–91. https://doi.org/10.1016/j.radonc.2016.07.007.